Polym. Bull. (2018) 75:4641–4655
https://doi.org/10.1007/s00289-018-2284-3

ORIGINAL PAPER

Facile fabrication of superhydrophobic nanocomposite coating using modified silica nanoparticles and non-fluorinated acrylic copolymer

Ali Pourjavadi[1] · Hamed Esmaili[1] · Mojtaba Nazari[1]

Received: 4 October 2017 / Revised: 20 January 2018 / Accepted: 27 January 2018 /
Published online: 12 February 2018

Abstract A superhydrophobic nanocomposite coating was fabricated using a simple procedure. The nanocomposite is composed of an acrylic copolymer and modified silica nanoparticles. The acrylic copolymer was prepared by free radical copolymerization of methyl methacrylate and dodeycl methacrylate monomers. Silica nanoparticles were synthesized and modified with an alkyl silane reagent, hexadecyltrimethoxysilane. A mixture of acrylic copolymer and modified silica nanoparticles, dispersed in dichloromethane, was then sprayed on glass and filter paper surface. Chemical composition and structure of the coatings were investigated by FTIR, FESEM, AFM, ^{1}H-NMR and GPC. The wettability of the prepared coating was examined by water contact angle measurement. The results showed that superhydrophobic surfaces with contact angle above 150° and rough structures were obtained. The prepared coatings also exhibited superoleophilic and self-cleaning properties.

Keywords Superhydrophobic · Nanocomposite coatings · Acrylic polymers · Self-cleaning · Silica nanoparticles

Introduction

Superhydrophobic surfaces are defined as surfaces with water contact angle greater than 150° [1]. This property was first observed in nature; for example, lotus leaves exhibit excellent water repellency on which the water droplets do not spread, but take a spherical shape and then can be easily rolled off [2]. Recently, these surfaces

✉ Ali Pourjavadi
purjavad@sharif.edu

[1] Polymer Research Laboratory, Department of Chemistry, Sharif University of Technology, Tehran, Iran

have attracted much attention both in academic research and practical applications due to their unique properties, such as water repellency, self-cleaning, anti-icing and anti-fouling [3–6].

It is now well known that superhydrophobicity arises from a combination of low surface free energy and surface roughness [7]. There are two general methods for fabrication of artificial superhyrophobic surfaces: roughening of hydrophobic surfaces and modifying the rough surfaces with low surface free energy materials. Different strategies including electrospinning [8], etching [9, 10], templating [11], layer-by-layer deposition [12], and photolithography [13] have been used to achieve rough surfaces. However, most of these methods are laborious or need complex processes or instruments. Other methods such as sol–gel and self-assembly process are simpler and seem to be more effective and practical for larger surfaces and industrial purposes [14, 15].

Using polymer nanocomposites is a simple and effective method to modify surface properties and achieve superhydrophobicity. The presence of nanoparticles in the polymer structure provides surface roughness with hierarchically micro- and nanostructures. Although a variety of nanoparticles such as silica [16], titanium dioxide [17] and zinc oxide [18] have been used for this purpose, silica nanoparticles are the most widely studied.

Fluorinated compounds have been recognized as appropriate materials for preparing superhydrophobic surfaces because of their low surface free energy [19, 20]. However, they are expensive and also it is difficult to use and functionalize them. Silicones are another class of polymers with low surface free energy that have been widely used for the preparation of superhydrophobic coatings [21, 22]. Other polymers such as polystyrene [23], polymethyl methacrylate (PMMA) and other acrylic polymers have been less frequently discussed in the literature [24].

The interfacial interaction between inorganic nanoparticles and polymer matrix is a very important parameter affecting the physical properties of the resulting nanocomposite. In the case of weak interfacial interaction, the nanoparticles separate easily from the polymer matrix and, as a result, a uniform and stable nanocomposite coating will not be obtained [25]. So, it is necessary to prepare a nanocomposite system with strong nanomaterial–polymer interfacial interaction. To fulfill this requirement, we fabricated a specific modified silica–polymer system in which the interaction of polymer and the nanoparticles is high enough to form a uniform and well-distributed silica coating. The composition of the polymer was designed in a way to provide the desired properties such as good adhesion and interaction with both nanoparticles and substrate.

The surface of silica nanoparticles was first modified with an alkyl silane reagent. A hydrophobic acrylic copolymer was also prepared. The coating was applied onto the substrate with simple spraying. A series of nanocomposite coatings was prepared combining the properties of both silica nanoparticles and acrylic polymers and the effect of nanocomposite composition on the wettabilty of the coating was studied to achieve optimum properties. Superhydrophobic surfaces with water contact angle greater than 150° and self-cleaning properties were obtained by this method.

Experimental

Reagents and methods

Tetraethylorthosilicate (TEOS) and hexadecyltrimethoxysilane (HDTMS) were purchased from Sigma-Aldrich and used as received. Methyl methacrylate (MMA) and dodecyl methacrylate (DMA) were purchased from Merck and distilled under reduced pressure before use. All other materials including dimethylformamide (DMF), ethanol, methanol, dichloromethane, ammonia (25%) and azobisisobutyronitrile (AIBN) were provided from Merck and used without further purifications.

Microscopic glass slides (26 × 76 mm) and filter papers (Whatman, number 42, 112 cm diameter) were used as substrate for coating. To clean the surface of the glass slides prior to coating, the glass slides were sonicated in ethanol, water and acetone, respectively, for 5 min. The glass slides were then treated with nitric acid solution (30%) for 30 min to remove surface contaminants and dust. Finally, the slides were rinsed with distilled water and dried in an oven at 50 °C.

Fourier-transform infrared (FTIR) spectra were recorded on a ABB Bomem MB 100 spectrophotometer. The samples were pressed into KBr pellets and the spectra were recorded in the region of 400–4000 cm^{-1}. Gel permeation chromatography (GPC) was carried out on an Agilent series 1100 instrument with cross-linked polystyrene-packed column. Tetrahydrofuran (THF) was used as eluent and the flow rate was fixed at 1 mL min^{-1}. The molecular weight and molecular weight distribution of the sample were determined using polystyrene standard samples. The polymer sample was dissolved in THF, filtered through filter paper and then injected into the instrument. Nuclear magnetic resonance (NMR) spectra were collected on a Bruker 500 MHz instrument. Samples were dissolved in $CDCl_3$, and tetramethylsilane (TMS) was used as internal standard. Field emission scanning electron microscopy (FESEM) images were taken by a Mira 3-XMU electron microscope. The samples were coated with a thin layer of gold film and then mounted onto the sample holder. Atomic force microscopy (AFM) was carried out using a Veeco instrument in non-contact mode. Contact angle measurements were performed by a ramé-hart Goniometer. 10 μl-sized droplets were used for the measurements and an average value of at least five readings was provided for each sample at room temperature. The image of the droplet was obtained by a Canon digital camera.

Synthesis of silica nanoparticles

50 mL ethanol and 2 mL water were poured in a round-bottom flask and 5 mL TEOS was added to it. The pH of the solution was adjusted to 10 using ammonia solution and the mixture was stirred at 50 °C for 5 h. Then, the flask was cooled to room temperature and the white solid product was centrifuged and washed with ethanol three times. The resulting silica nanoparticles were dried at 50 °C.

Surface modification of silica nanoparticles

0.5 g of the synthesized silica nanoparticles was dispersed in 50 mL ethanol:water mixture (4:1) in a round-bottom flask and sonicated for 20 min. Then, 4 mL HDTMS was added and the pH of the mixture was adjusted to 10 using ammonia solution. The flask was equipped with a condenser and a magnetic stirrer and was heated at 75 °C for 12 h. Afterward, the flask was cooled to room temperature and its content was filtered and washed three times with ethanol. The white solid product was dried in an oven at 50 °C.

Preparation of poly(MMA-*co*-DMA)

15 mL DMF was poured in a round-bottom flask equipped with a condenser and a magnetic stirrer. Then, 2 g MMA, 2 g DMA and 0.08 g AIBN were added and the flask was put in an oil bath. The reaction was performed at 70 °C for 12 h. After cooling to room temperature, the mixture was poured into 30 mL methanol as non-solvent. The precipitated copolymer was washed several times with methanol and dried in an oven at 50 °C.

Coating on the surface

A certain amount of poly(MMA-*co*-DMA) was dissolved in 30 mL dichloromethane. Then, modified silica nanoparticles were added and the mixture was sonicated for 10 min. The mixture was coated onto the surface using an ordinary spray device. The coated surfaces were then dried at ambient temperature for 15 min.

Results and discussion

Nanocomposite coatings were prepared by spraying a mixture of HDTMS-modified silica nanoparticles and poly(MMA-*co*-DMA). The neat silica nanoparticles are covered with hydroxyl groups on their surface. So, we modified it with long chain alkyl groups (Fig. 1) to increase their hydrophobicity and compatibility with the hydrophobic acrylic copolymer.

The acrylic copolymer prepared here is composed of MMA and DMA. Acrylic polymers usually show good adhesion to different substrates and have good film-

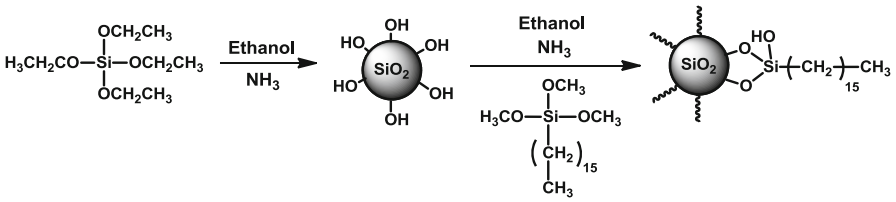

Fig. 1 Synthesis and surface modification of silica nanoparticles

forming properties. In acrylic polymers, the T_g of the polymer decreases as the length of the alkyl side chain increases. The homopolymer of MMA has T_g above 100 °C which is relatively high [26]. Thus, we used DMA as a comonomer to decrease T_g of the polymer and increase flexibility and adhesion of polymer to the substrate. The long alkyl chain of DMA provides more hydrophobicity for the prepared copolymer and also for the final coating. The synthesis reaction and structure of poly(MMA-*co*-DMA) is depicted in Fig. 2.

The final nanocomposite coatings were fabricated by spraying a mixture of HDTMS-modified nanoparticles and poly(MMA-*co*-DMA), dispersed in dichloromethane, on the substrate surface. The schematic route for preparation of nanocomposites is illustrated in Fig. 3.

Characterization and wettability

The surface of many materials such as glass, paper and wood is normally hydrophilic due to the presence of different hydrophilic functional groups such as hydroxyl groups. As a consequence, the water droplet tends to spread and wet these

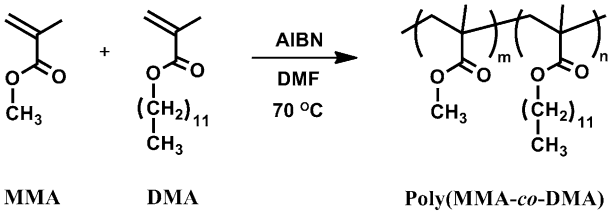

Fig. 2 Synthesis of poly(MMA-*co*-DMA)

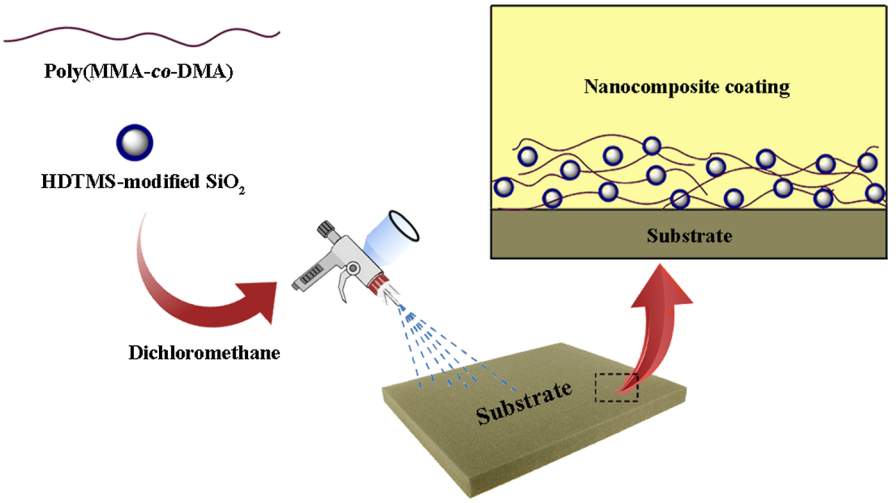

Fig. 3 The schematic route for preparation of nanocomposite coatings

surfaces. However, covering these surfaces with a rough structure of a hydrophobic coating decreases its hydrophilicity. Hydrophobic polymers with good film-forming properties, flexibility and optical transparency are more desired. Among different polymeric materials, acrylic polymers are characterized as polymers possessing appropriate properties to be used for coating.

The coating prepared here is composed of an acrylic copolymer in which the modified silica nanoparticles are dispersed. Although silica nanoparticles are the most widely inorganic material used for fabrication of superhydrophibic coatings, they are hydrophilic and, thus, their surface needs to be modified with hydrophobic materials [27]. FTIR spectrum of silica nanoparticles (Fig. 4a) shows two main peaks at 3300 and 1100 cm^{-1} which are attributed to O–H and Si–O–Si stretching vibrations, respectively. The presence of a wide strong OH absorption band indicates the hydrophilic nature of these nanoparticles. The new peaks that appeared at 2856 and 2927 cm^{-1} in the spectrum of HDTMS-modified silica (Fig. 4b) are attributed to C–H stretching vibrations of alkyl chains and confirms that the silica nanoparticles were successfully modified with hydrophobic silane reagent.

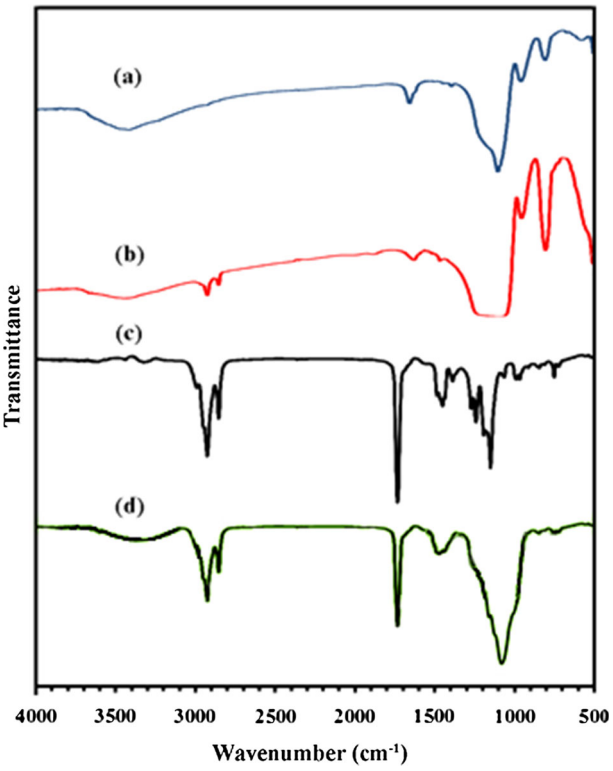

Fig. 4 FTIR spectra of **a** silica, **b** HDTMS-modified silica, **c** poly(MMA-*co*-DMA) and **d** sprayed-coated nanocomposite

FTIR spectrum of poly(MMA-*co*-DMA) (Fig. 4c) shows sharp peaks at 1731 and 1149 cm^{-1} which are characteristic peaks of ester carbonyl and C–O groups, respectively. The peaks that appeared at 2852 and 2925 cm^{-1} are related to C–H stretching vibrations. In the FTIR spectrum of the nanocomposite (Fig. 4d), a new peak is also observed at 1100 cm^{-1} which is a characteristic peak of the Si–O–Si groups and confirms the formation of modified silica/acrylic composite.

FESEM images of silica and modified silica nanoparticles are shown in Fig. 5. Silica nanoparticles are semispherical and nearly monodisperse with sizes about 30–50 nm (Fig. 5a). In FESEM image of HDTMS-modified silica nanoparticles (Fig. 5b), there is only a small increase in the size and aggregation of the nanoparticles, and no significant morphological difference is observed.

To evaluate the coatings, first, the synthesized acrylic copolymers without any nanoparticles were coated on the glass substrate using the spray method. It was observed that a uniform thin and transparent film was formed on the glass surface. The prepared acrylic coating had also a very good adhesion to the surface resulting in a stable and durable coating. Molecular weight and molecular weight distribution of poly(MMA-*co*-DMA) were determined by GPC and the related diagram is depicted in Fig. 6. Weight-average molecular weight ($\bar{M}_w$) and number-average molecular weight ($\bar{M}_n$) of the polymer are 6.41×10^4 g mol^{-1} and 2.53×10^4, respectively, and its polydispersity index (PDI) is 2.53.

The ^{1}H-NMR spectrum and the chemical structure of poly(MMA-*co*-DMA) are shown in Fig. 7. The signals corresponding to each proton present in the structure of poly(MMA-*co*-DMA) chains are also assigned in this figure. The signal at 1.29 ppm corresponds to ten protons of the methylene groups present in the DMA units (protons assigned as e). The signals at 1.63 and 1.82 ppm are ascribed to the protons in the methylene groups present in the main chain (protons assigned as a) and protons in methyl groups of meta position (protons assigned as b), respectively. The

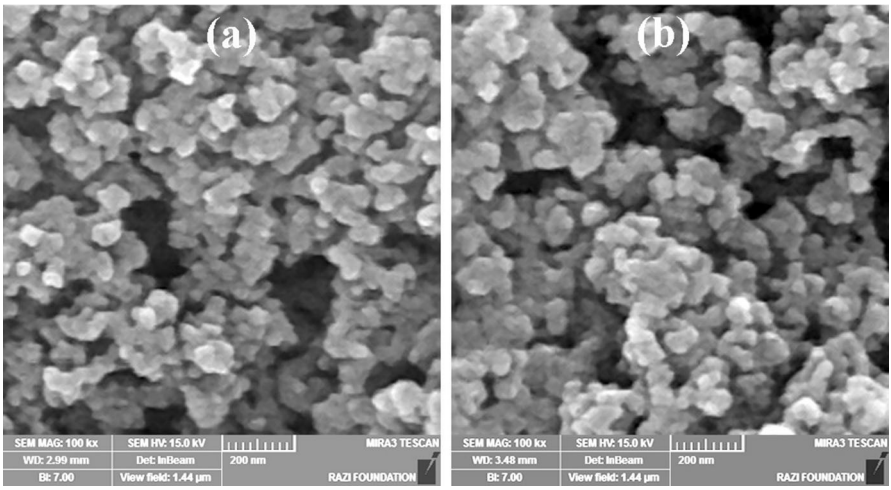

Fig. 5 FESEM images of **a** silica and **b** HDTMS-modified silica

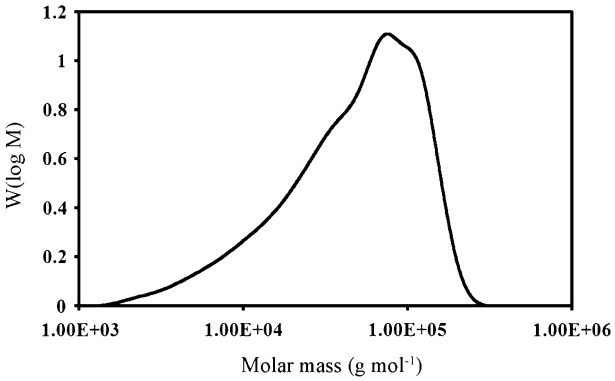

Fig. 6 Gel permeation chromatogram of poly(MMA-*co*-DMA)

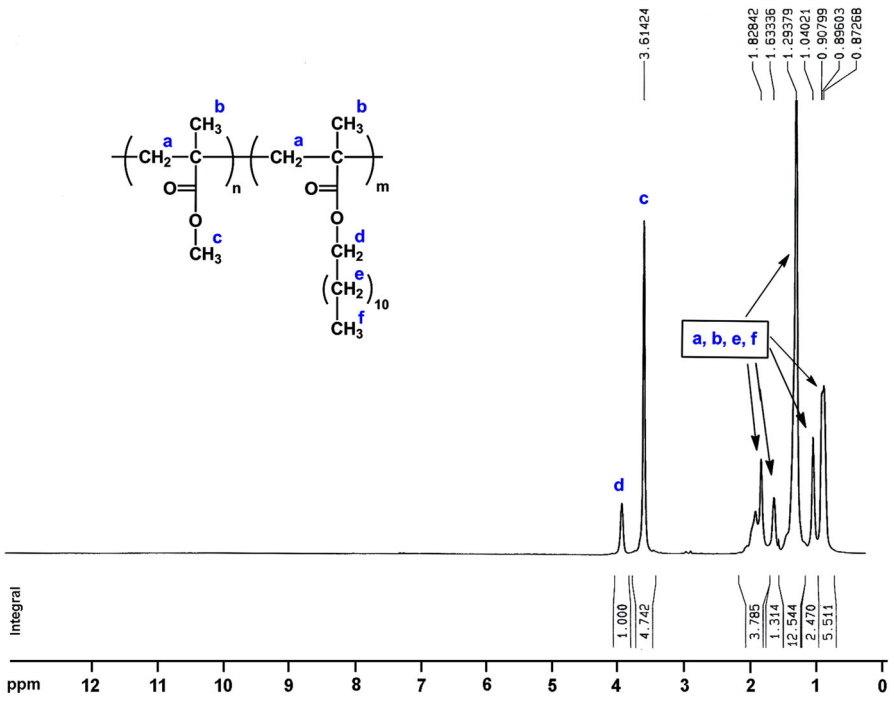

Fig. 7 ^{1}H-NMR spectrum of poly(MMA-*co*-DMA)

chemical shifts at 3.6 and 4 ppm corresponds to protons of methylene groups which are adjacent to the ester groups of MMA and DMA (protons assigned as c and d), respectively.

The chemical composition of the poly(MMA-*co*-DMA) was then determined from ^{1}H-NMR spectrum. The molar fraction of the two monomers in the copolymer chain was calculated according to the following equation:

$$f_{\mathrm{MMA}} = \frac{\frac{I_c}{n_c}}{\frac{I_c}{n_c} + \frac{I_d}{n_d}} \times 100, \quad (1)$$

where f_{MMA} is the molar ratio of MMA, I_c and I_d are the total integration of the signals at chemical shifts of 3.6 and 4 ppm, respectively, and n_c and n_d are the number of hydrogens assigned to related groups of each monomer (hydrogens assigned as c and d, respectively). The calculation revealed that the molar fractions of MMA and DMA units in the acrylic copolymer are 0.83 and 0.17, respectively.

In spite of its good optical and physical properties, the coated acrylic copolymer does not have enough hydrophibicity as is desired. The water contact angle of the acrylic copolymer is only 92° which is far lower than that of a superhydrophobic surface. FESEM image of poly(MMA-*co*-DMA) shows that the copolymer has a smooth surface without any significant roughness (Fig. 8b). Although this surface morphology is appropriate in forming a uniform thin coating, it does not have enough structural requirements for a superhydrophobic surface.

Then, we prepared coatings with various weight percentages of modified silica nanoparticles on the glass surface. The water contact angle of nanocomposites containing 40, 60 and 80 wt% of modified silica nanoparticles was found to be 142°, 152°, and 155°, respectively. Thus, superhydrophobicity was obtained in nanocomposites with nanoparticle percentages higher than 60 wt%.

As shown in Fig. 8c, the prepared nanocomposite coating has significant roughness which is due to the presence of modified silica nanoparticles (Fig. 8a).

These results indicate that the optimum ratio of modified silica nanoparticles to poly(MMA-*co*-DMA) is 60:40. Also, the filter paper coated with this nanocomposite exhibited a water contact angle of 153°. The water droplets take a spherical shape and do not wet these surfaces. With higher percentages of modified silica nanoparticles, no homogenous and stable films were formed. The water contact angle of the prepared coating is shown in Fig. 9.

The surface free energy and surface roughness are two important factors that determine the wettability of the surfaces. The wettability of the surfaces can be

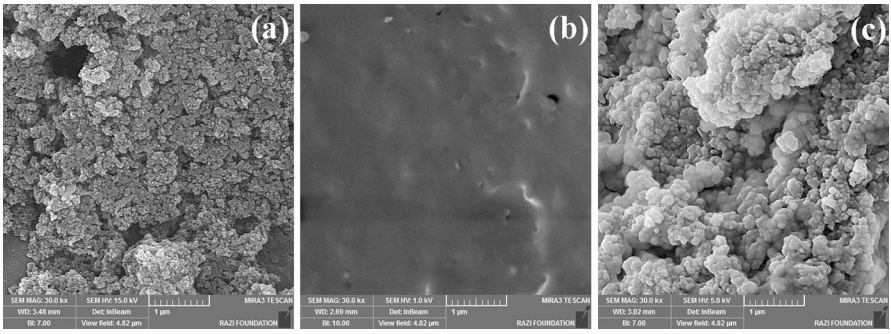

Fig. 8 FESEM images of **a** HDTMS-modified silica, **b** poly(MMA-*co*-DMA) and **c** nanocomposite coating

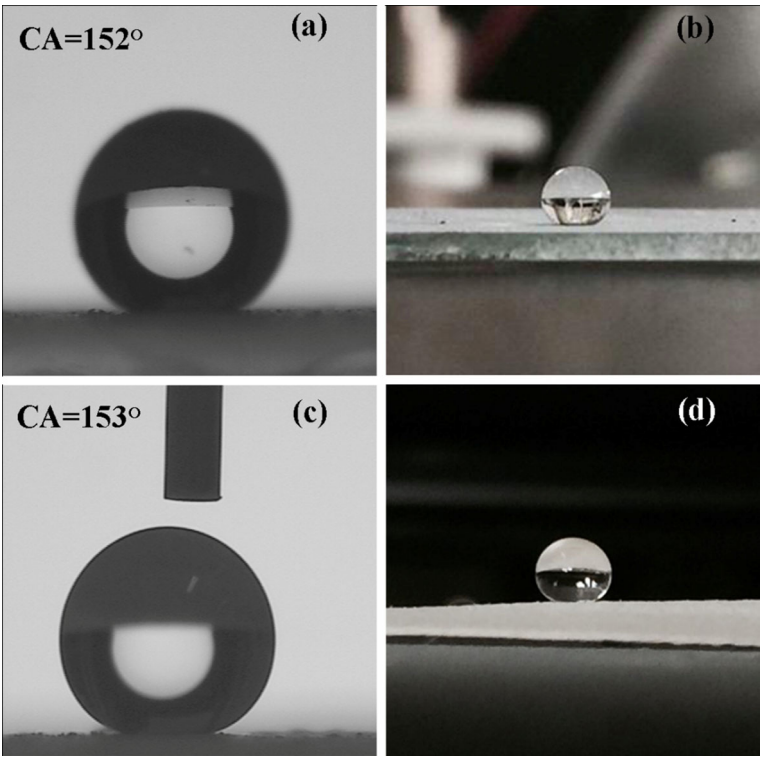

Fig. 9 Water contact angle of **a** glass and **c** filter paper, and photograph of water droplet on **b** glass and **d** paper, all coated with nanocomposite containing 60 wt% HDTMS-modified silica nanoparticles

described by different theoretical models, one of which is the Young model expressed as follows [28]:

$$\cos\theta = \frac{\gamma_{SV} - \gamma_{SL}}{\gamma_{LV}}, \tag{2}$$

where, γ_{LV}, γ_{SL} and γ_{LV} are liquid–vapor, solid–liquid and solid–vapor interfacial free energy, respectively. In the Young model, the water contact angle is only dependent on interfacial energies acting between different interfaces and surfaces with lower surface free energies have higher water contact angles. However, this model is only valid for flat, smooth and chemically homogenous surfaces.

The wettability of the rough surfaces is usually described by Wenzel and Cassie–Baxter models. The Wenzel model assumes that the water is completely in contact with the whole solid surface below it. The Cassie–Baxter model assumes that the water is in contact only with the top of the rough surface and air is trapped in the grooves under the water droplet.

The Wenzel model is expressed as follows [29]:

$$\cos\theta_r = r\cos\theta, \tag{3}$$

where r is the roughness factor ($r \geq 1$, with $r = 1$ for smooth surfaces) and θ and θ_r are the water contact angles for smooth and rough surfaces, respectively. According to this equation, when θ is lower than 90°, increase in the surface roughness decreases θ_r. In contrast, when θ is higher than 90°, increase in the surface roughness increases θ_r.

The Cassie–Baxter model is expressed as follows [30]:

$$\cos\theta_r = f_1\cos\theta - f_2, \tag{4}$$

where θ and θ_r are the water contact angles for the smooth and rough surfaces, respectively, and f_1 and f_2 are the area fractions of the surface and air in contact with water, respectively (i.e., $f_1 + f_2 = 1$). According to this equation, roughening the surface increases the water contact angles.

Surface topography of the prepared nanocomposite coating was also investigated by AFM. As shown in Fig. 10, the surface of the coating is rough which is in accordance with FESEM observations. According to the Wenzel and Cassie–Baxter models, this surface roughness along with hydrophobic nature (low surface free energy) of the prepared coatings is the reason for the observed superhydrophobic behavior.

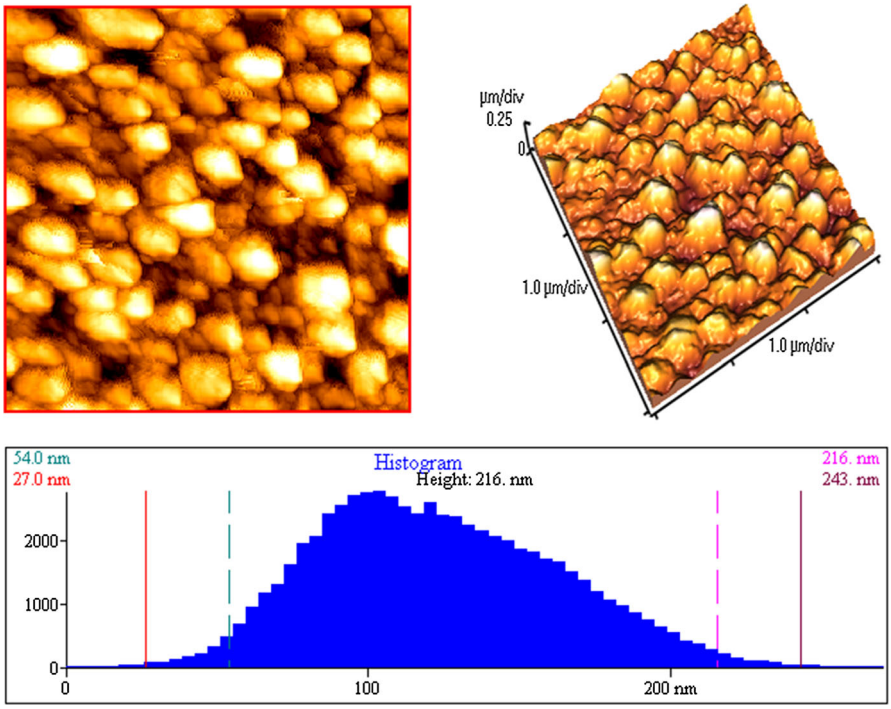

Fig. 10 AFM images and thickness profile of the prepared coating on the glass surface

Surface composition and microstructure are considered to be two factors affecting the wettability of the surface. When HDTMS-modified SiO_2 nanoparticles are dispersed in the solution, some degree of aggregation occurs between these nanoparticles. When the suspension is sprayed over the surface of the substrate, the solvent evaporates and an aggregation of the nanometer-sized modified silica nanoparticles is formed, in which void spaces also exist. It is believed that this aggregation causes the surface of the coatings to be rough [15]. In addition to the aggregation, the size of the particles affects the wettability of the resulting coating. More superhydrophibicity is obtained with smaller particle sizes. According to these results, the superhydrophobic coating obtained in this study is the result of a combination of parameters including surface modification, nanometer-sized particles and surface roughness.

The photographs of water and oil droplets on the prepared coatings are shown in Fig. 11. For better visualization, the water and oil droplets were dyed with blue and red colors, respectively. It is observed that the water droplets are in the form of sphere and do not spread and wet the surface. In contrast, the oil droplet completely and immediately spreads and wets the surface. As reported in the literature, this property can be used for the separation of oil from water, especially when the material is in the form of foam, sponge and paper [31–33].

Self-cleaning behavior

Graphite powder as dirt particles was spread over the surface of the coated glass. Then, water droplets were placed on the coating and slowly rolled back and forth over the coating to collect the dirt particles. As shown in Fig. 12, the dirt particles were almost completely adsorbed on the water droplets and removed from the surface. It is also observed that the water droplets preserve their ball-like spherical shape even after adsorption of dirt particles. The results show that in addition to its water repellency and superoleophilicity, the prepared coating exhibits self-cleaning properties.

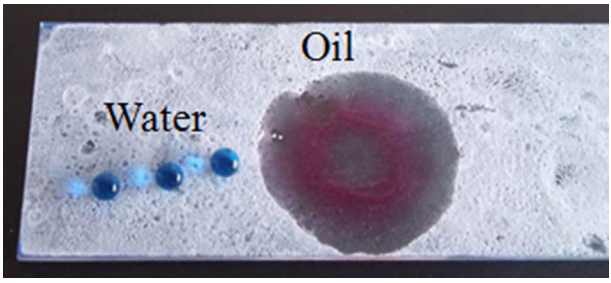

Fig. 11 The photographs of water and oil droplets on the prepared coatings

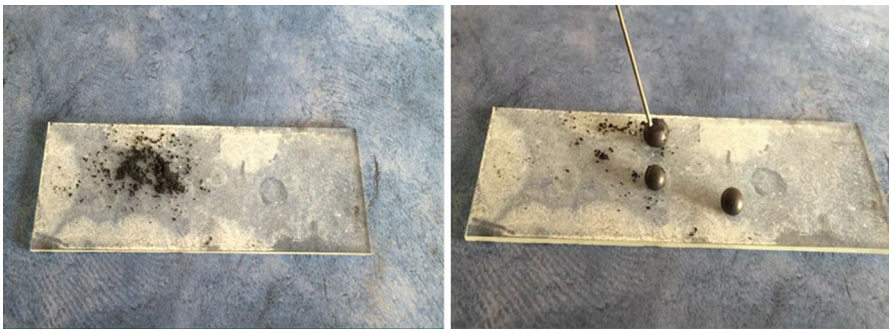

Fig. 12 Self-cleaning behavior of the prepared coating

Conclusion

In conclusion, we prepared nanocomposite coatings on glass and filter paper surface by spraying a mixture of modified silica nanoparticles and poly(MMA-*co*-DMA) in dichloromethane. Modification of silica nanoparticles with HDTMS lowered the surface free energy of the nanoparticles and increased their compatibility with hydrophobic acrylic copolymer. The prepared coating had a rough surface morphology with micro- and nanostructure. Increasing the modified silica content increased water contact angle and the best result was obtained with 60:40 composition of modified silica to polymer. The presence of poly(MMA-*co*-DMA) is necessary to assure the adhesion of these nanoparticles to the substrate. The highest water contact angle on these surfaces was 153°, indicating that the prepared coatings were superhydrophobic. The prepared coating also exhibited self-cleaning behavior, being able to remove dirt from its surface. The results confirm the importance of surface modification, chemical structure, nanoparticle to polymer ratio and other experimental conditions which should be considered for fabrication of such nanocomposite coatings.

References

1. Ganesh VA, Raut HK, Nair AS et al (2011) A review on self-cleaning coatings. J Mater Chem 21(41):16304–16322
2. Guo Z, Liu W, Su BL (2011) Superhydrophobic surfaces: from natural to biomimetic to functional. J Colloid Interface Sci 353(2):335–355
3. Ruan M, Li W, Wang B et al (2013) Preparation and anti-icing behavior of superhydrophobic surfaces on aluminum alloy substrates. Langmuir 29(27):8482–8491
4. Xue CH, Guo XJ, Ma JZ et al (2015) Fabrication of robust and antifouling superhydrophobic surfaces via surface-initiated atom transfer radical polymerization. ACS Appl Mater Interfaces 7(15):8251–8259
5. Wang H, Liu Z, Zhu Y et al (2016) Facile preparation of superhydrophobic and high oleophobic polymer composite coatings with self-cleaning, heat-resistance and wear-resistance. J Polym Res 23(7):1–9

6. Cao M, Guo D, Yu C et al (2015) Water-repellent properties of superhydrophobic and lubricant-infused "slippery" surfaces: a brief study on the functions and applications. ACS Appl Mater Interfaces 8(6):3615–3623
7. Yan YY, Gao N, Barthlott W (2011) Mimicking natural superhydrophobic surfaces and grasping the wetting process: a review on recent progress in preparing superhydrophobic surfaces. Adv Colloid Interface Sci 169(2):80–105
8. Oktay B, Toker RD, Kayaman-Apohan N (2015) Superhydrophobic behavior of polyimide–siloxane mats produced by electrospinning. Polym Bull 72(11):2831–2842
9. Liao R, Zuo Z, Guo C et al (2014) Fabrication of superhydrophobic surface on aluminum by continuous chemical etching and its anti-icing property. Appl Surf Sci 317:701–709
10. Xie L, Tang Z, Jiang L et al (2015) Creation of superhydrophobic wood surfaces by plasma etching and thin-film deposition. Surf Coat Technol 281:125–132
11. Peng P, Ke Q, Zhou G et al (2013) Fabrication of microcavity-array superhydrophobic surfaces using an improved template method. J Colloid Interface Sci 395:326–328
12. Zhang C, Zhang S, Gao P et al (2014) Superhydrophobic hybrid films prepared from silica nanoparticles and ionic liquids via layer-by-layer self-assembly. Thin Solid Films 570:27–32
13. Sung YH, Kim YD, Choi HJ et al (2015) Fabrication of superhydrophobic surfaces with nano-in-micro structures using UV-nanoimprint lithography and thermal shrinkage films. Appl Surf Sci 349:169–173
14. Mahadik SA, Vhatkara RS, Mahadik DB et al (2013) Superhydrophobic silica coating by dip coating method. Appl Surf Sci 277:67–72
15. Ogihara H, Xie J, Okagaki J et al (2012) Simple method for preparing superhydrophobic paper: spray-deposited hydrophobic silica nanoparticle coatings exhibit high water-repellency and transparency. Langmuir 28(10):4605–4608
16. Mahadik SA, Fernando PD, Hegade ND et al (2013) Durability and restoring of superhydrophobic properties in silica-based coatings. J Colloid Interface Sci 405:262–268
17. Wang Y, Li B, Liu T et al (2014) Controllable fabrication of superhydrophobic TiO_2 coating with improved transparency and thermostability. Colloids Surf A 441:298–305
18. Liu Z, Wang H, Wang E et al (2016) Superhydrophobic poly (vinylidene fluoride) membranes with controllable structure and tunable wettability prepared by one-step electrospinning. Polymer 82:105–113
19. Ye Z, Chen Y, Yang X et al (2017) Development of perfluoropolyether modified raspberry particles with fine hierarchical structure and their application in superhydrophobic surface. Colloids Surf 514:251–259
20. Yang H, Pi P, Yang ZR et al (2016) Design of a superhydrophobic and superoleophilic film using cured fluoropolymer@silica hybrid. Appl Surf Sci 388:268–273
21. Chu Z, Seeger S (2015) Robust superhydrophobic wood obtained by spraying silicone nanoparticles. RSC Adv 5(28):21999–22004
22. Yuan R, Wu S, Wang H et al (2017) Facile fabrication approach for a novel multifunctional superamphiphobic coating based on chemically grafted montmorillonite/Al_2O_3-polydimethylsiloxane binary nanocomposite. J Polym Res 24(4):59
23. Neto AI, Meredith HJ, Jenkins CL et al (2013) Combining biomimetic principles from the lotus leaf and mussel adhesive: polystyrene films with superhydrophobic and adhesive layers. RSC Adv 3(24):9352–9356
24. Ma Y, Cao X, Feng X et al (2007) Fabrication of super-hydrophobic film from PMMA with intrinsic water contact angle below 90. Polymer 48(26):7455–7460
25. Guo YG, Jiang D, Zhang Zhang X et al (2010) Room temperature synthesis of water-repellent polystyrene nanocomposite coating. Appl Surf Sci 256(23):7088–7090
26. Porter CE, Blum FD (2000) Thermal characterization of PMMA thin films using modulated differential scanning calorimetry. Macromolecules 33(19):7016–7020
27. Gurav AB, Xu Q, Latthe SS et al (2015) Superhydrophobic coatings prepared from methyl-modified silica particles using simple dip-coating method. Ceram Int 41(2):3017–3023
28. Young T (1805) An essay on the cohesion of fluids. Philos Trans R Soc Lond B Biol Sci 95:65–87
29. Wenzel RN (1936) Resistance of solid surfaces to wetting by water. Ind Eng Chem 28(8):988–994
30. Cassie A, Baxter S (1944) Wettability of porous surfaces. Trans Faraday Soc 40:546–551
31. Zhu Q, Chu Y, Wang Z et al (2013) Robust superhydrophobic polyurethane sponge as a highly reusable oil-absorption material. J Mater Chem A 1(17):5386–5393

32. Ge B, Zhang Z, Zhu X et al (2014) A superhydrophobic/superoleophilic sponge for the selective absorption oil pollutants from water. Colloids Surf A 457:397–401
33. Peng L, Lei W, Yu P et al (2016) Polyvinylidene fluoride (PVDF)/hydrophobic nano-silica (H–SiO_2) coated superhydrophobic porous materials for water/oil separation. RSC Adv 6(13):10365–10371